

Highlights:

- Rapid and sensitive direct injection method for analysis of seven target ICMs
- The method was validated in complex aqueous matrices such as secondary effluent, groundwater and drinking water
- Removal of seven target ICMs by LPUV/H₂O₂, LPUV/Cl₂ and LPUV/NH₂Cl

**A direct injection liquid chromatography tandem mass spectrometry
method for the kinetic study on iodinated contrast media (ICMs)
removal in natural water**

Authors: Israel J. Lopez-Prieto^a, Shimin Wu^{a,b}, Weikang Ji^a, Kevin D. Daniels^{a,c}, and
Shane A. Snyder^{a,d}

^aUniversity of Arizona, Department of Chemical & Environmental Engineering, 1133 E.
James E Rogers Way, Harshbarger 108, Tucson, AZ 85721-0011, United States

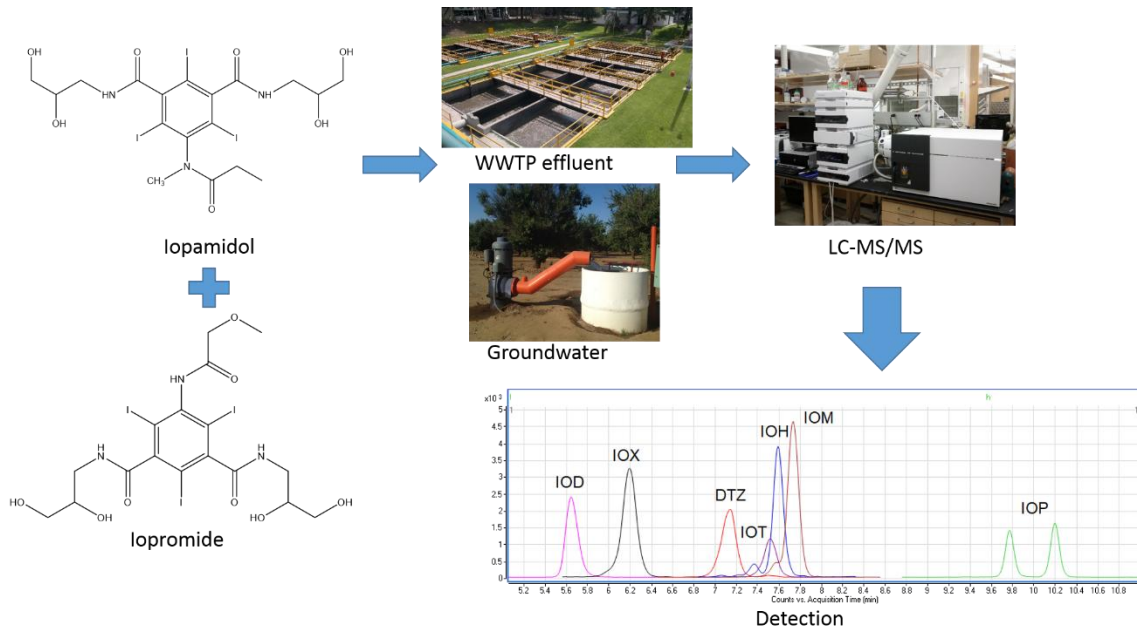
^bEREnvironmentalProtectionEngineeringTechnologyCo., Ltd., Shenzhen 518071, China

^cHazen and Sawyer, 1400 E. Southern Avenue, Suite 340, Tempe, AZ 85282, United
States

^dNanyang Technological University, Nanyang Environment & Water Research Institute,
Clean Tech One, 1 Cleantech Loop, #06-08, Singapore 637141, Singapore

Corresponding author, email: ssnyder@ntu.edu.sg

Graphical abstract



1 **A direct injection liquid chromatography tandem mass spectrometry**
2 **method for the kinetic study on iodinated contrast media (ICMs)**
3 **removal in natural water**

4 Authors: Israel J. Lopez-Prieto^a, Shimin Wu^{a,b}, Weikang Ji^a, Kevin D. Daniels^{a,c}, and
5 Shane A. Snyder^{a,d}.

6
7 ^aUniversity of Arizona, Department of Chemical & Environmental Engineering, 1133 E.
8 James E Rogers Way, Harshbarger 108, Tucson, AZ 85721-0011, United States

9 ^bEREnvironmentalProtectionEngineeringTechnologyCo., Ltd., Shenzhen 518071, China

10 ^cHazen and Sawyer, 1400 E. Southern Avenue, Suite 340, Tempe, AZ 85282, United
11 States

12 ^dNanyang Technological University, Nanyang Environment & Water Research Institute,
13 Clean Tech One, 1 Cleantech Loop, #06-08, Singapore 637141, Singapore

14
15 Corresponding author, email: ssnyder@ntu.edu.sg

16
17 **Abstract**

18 Iodinated contrast media (ICMs) are a class of X-ray contrast media worldwide utilized
19 for radiographic procedures. Since they cannot be removed efficiently during water
20 treatment, they can be found in surface and groundwater. In this work, a rapid and
21 sensitive direct injection liquid chromatography-tandem (LC-MS/MS) method for the
22 simultaneous analysis of seven ICMs media (iopamidol, ioxitalamic acid, diatrizoic
23 acid, iothalamic acid, iohexol, iomeprol and iopromide) in complex aqueous matrices
24 has been developed and validated. The MDLs for the analytes ranged from 0.7 to 21 ng
25 L⁻¹ in ultrapure water, and recoveries ranged from 86 to 100% in drinking water, 85 to

26 103% in groundwater and 84 to 105% in WWTP effluent. A stereo-isomer for
27 iopromide was separated. This analytic method was applied to investigate the removal
28 of target ICMs by low pressure ultra violet light (LPUV) advanced oxidation processes
29 with three oxidants, hydrogen peroxide, free chlorine and monochloramine in
30 groundwater. Results showed that the addition of oxidants did not enhance attenuation
31 of ICMs, since fluence-based decay apparent rate constants were similar ($K_{UV} = 3.2 \times 10^{-3}$
32 3 , $K_{UV-Cl_2} = 3.6 \times 10^{-3}$ and $K_{UV-NH_2} = 3.4 \times 10^{-3} \times 10^{-3} \text{ cm}^2 \text{ mJ}^{-1}$). This yielded direct photolysis
33 is the main mechanism to attenuate target ICMs.

34

35 **Keywords:** Iodinated contrast media, Direct injection, Liquid chromatography-tandem mass
36 spectrometry, Complex aqueous matrices, UV-based oxidation processes

37

38 1. Introduction

39

40 A current major challenge for water analysis is to develop a simple, sensitive and robust
41 method for the detection and quantification of emerging contaminants at trace levels in
42 complicated matrices such as surface water and wastewater effluents. In recent years,
43 iodinated contrast media (ICMs) as the most widely administered intravascular
44 pharmaceuticals in medical X-ray have become one of the most prevalent emerging
45 contaminants. Owing to their high polarity and biological stability, ICMs are usually
46 difficult to remove by conventional wastewater treatment (Busetti et al., 2008; Pauwels
47 & Verstraete, 2006). Hence ICMs have been detected at $\mu\text{g L}^{-1}$ levels in aqueous
48 environments, including surface water, groundwater, and even drinking water (Ternes
49 and Hirsch 2000; Weissbrodt et al. 2009). Although ICMs are non-toxic to the human
50 body, they have received increasing attention as potential precursors of iodinated
51 disinfection by-products (I-DBPs) which have been proven to be highly cytotoxic and

52 genotoxic to mammalian cells (Duirk et al., 2011). It has been reported in recent years
53 that I-DBPs are generally of much higher developmental toxicity and growth inhibition
54 than their bromo- and chloro-analogues (Richardson et al., 2008). There are two types
55 of ICMs based on their charges at a neutral pH. Non-ionic ICMs have been more
56 heavily studied than ionic ones since they are more abundant in surface waters (Pérez &
57 Barceló, 2007; Westerhoff et al., 2005). The most common methods involve liquid
58 chromatography coupled to an ultra violet detector (LC-UV) or tandem mass
59 spectrometry (LC-MS/MS). Tian et al., (2014) developed a method utilizing LC-UV
60 detector for quantification of iopamidol, with a detection limit of $5\mu\text{g L}^{-1}$. Ternes &
61 Hirsch (2000) developed a sensitive LC-MS/MS method with solid-phase extraction
62 (SPE) step using a non-polar cartridge and achieved a level of quantification of 10 ng L^{-1} .
63 In addition, Sacher et al., (2005) developed a method to analyze six ICMs using ion
64 chromatography (IC) for separation and inductively coupled plasma mass spectrometry
65 (ICP-MS) for quantification which obtains limits of detection of about $0.2\mu\text{g L}^{-1}$
66 without pre-concentration. Table 1 shows a summary of different methods developed
67 for ICM quantification.

68 Most current analytical methods for the determination of ICMs in aqueous matrices
69 include a SPE as a pre-concentration step in order to enrich the analytes, clean them up
70 from the interfering matrices, and achieve lower detection limits (Ternes et al., 2005).
71 However, SPE procedure is costly and time-consuming, and may result in a loss of
72 analytes (Sacher & Brauch, 2005). Large volume injection LC-MS/MS methods have
73 become popular since they do not require a pre-concentration step with SPE. They also
74 increase the overall recoveries of the analysis, whereas achieve lower limits of detection
75 (LOD) (Tarun A. et al., 2013).

76 The objective of this study was to develop a rapid, sensitive and robust direct injection
77 LC-MS/MS method for the simultaneous analysis of seven ICMs (iopamidol,
78 ioxitalamic acid, diatrizoic acid, iothalamic acid, iohexol, iomeprol and iopromide) in
79 environmental waters such as secondary effluent, ground water and drinking water. This
80 current method was applied to investigate the removal of target ICMs by low pressure
81 ultra violet (LPUV) advanced oxidation processes with three oxidants (hydrogen
82 peroxide, free chlorine and monochloramine) in groundwater.

83

84 **[Table 1]**

85

86 **2. Materials and methods**

87

88 **2.1. Chemicals**

89

90 Diatrizoic acid (DTZ) was purchased from Sigma-Aldrich (St. Louis, MO, USA).
91 iothalamic acid (IOT) and ioxitalamic acid (IOX) were purchased from Toronto
92 Research Chemicals (Ontario, Canada). Iohexol (IOH), iopamidol (IOD), and iopromide
93 (IOP) were obtained from the United States Pharmacopeial Convention Inc. (Rockville,
94 MD, USA). Iomeprol (IOM) was purchased from LGC Standards (Manchester, NH,
95 USA). The isotopically labeled surrogate standards (ILSS), iohexol-d₅ (IOH-d₅) and
96 iopamidol-d₃ (IOD-d₃), were also obtained from Toronto Research Chemicals (Ontario,
97 Canada) LC/MS grade methanol, acetonitrile, formic acid and acetic acid were
98 purchased from Fisher Scientific Co. (Fair Lawn, NJ, USA). Ammonium acetate
99 (NH₄Ac) and ammonium formate (NH₄Fo) were obtained from Sigma-Aldrich (St.

100 Louis, MO, USA). Ultrapure water with a resistivity of 18.1 M Ω ·cm was obtained from
101 a Milli-Q system (Millipore, Billerica, MA).

102 Stock solutions of each target ICM and isotope surrogate standard were prepared at 1.0
103 mg mL⁻¹ in methanol. A standard mix (sub-stock solution) of all the analytes at 10 μ g
104 mL⁻¹ and of the two isotopically labeled surrogates at 1.0 μ g mL⁻¹ were prepared in
105 methanol. Working standard solutions at concentrations of 10, 20, 50, 100, 200, 500,
106 1000, 2000, 5000, 10000 and 20000 ng L⁻¹ were prepared weekly by serially diluting
107 the mixed sub-stock solution of analytes in methanol, and then spiking ILSS at 1000 ng
108 L⁻¹ afterward. Stock solutions were stored in the freezer at -20 °C.

109

110 **2.2. Sample collection and preparation**

111

112 Groundwater samples were collected from two monitoring wells downstream the
113 WWTP outfall. WWTP effluent was collected after secondary treatment to prior
114 chlorination basin. Drinking water from the university tap water was collected as well.
115 All samples were collected in 1 L amber glass bottles, which were rinsed with methanol
116 and ultrapure water and pre-baked at 400 °C prior to collection and stored at 4 °C for a
117 maximum of two weeks before analysis.

118 A 1000 ng L⁻¹ of ILSS mixture was spiked into one mL of each water sample. The
119 samples were then filtered with a 0.2 μ m pore size polyethylene sulfonate (PES) syringe
120 filter from Agilent Technologies (Palo Alto, CA) and placed in an autosampler vial for
121 analysis.

122

123 **2.3. Instrumentation**

124

125 The LC separation was carried out using an Agilent 1290 UHPLC system (Agilent
126 Technologies, Palo Alto, CA). Separation was conducted with an Agilent Poroshell 120
127 EC-C8 column (4.6×100 mm, 2.7 µm particle size) maintained at 30 °C with a constant
128 flow rate of 0.5 mL/min. Ultrapure water containing 0.1% (v/v) formic acid (A) and
129 methanol containing 0.1% (v/v) formic acid (B) were used as the mobile phases. The
130 gradient was as follows: B was initiated at 2%, and linearly increased to 20% in 8.0
131 min, then increased to 100% in 0.5 min and held for 2.5 min. A 4.0 min equilibration at
132 2% B was used at the end of each run. The injection volume was 80 µL.

133 Mass spectrometric detection was performed utilizing an Agilent 6490 triple quadrupole
134 mass spectrometer (Agilent Technologies, Palo Alto, CA) equipped to a Jet Stream dual
135 electrospray source and iFunnel technology. The instrument was tuned and optimized to
136 obtain adequate sensitivity and resolution using the Agilent tune solution (p/n: G1969-
137 85000) in all peak windows. The instrument was conducted utilizing an electrospray
138 ionization source (ESI) in positive mode, with optimized parameters as follows: gas
139 temperature, 275°C; gas flow, 18 L/min; sheath gas temperature, 350°C; sheath gas
140 flow, 12 L min⁻¹; nebulizer, 45 psi; fragmentor, 380 V. The optimized MRM transition
141 parameters for target ICMs and surrogate standards are listed in Table 2.

142

143 **[Table 2]**

144

145 **2.4. Identification and quantification**

146

147 Identification of the target ICMs was succeeded by comparing the retention time and the
148 relative intensities (RI) of the two detected product ions (Table 2). The tolerance of
149 relative retention time (RRT) was ±2%. The tolerances for various RIs were as follows:

150 $\pm 20\%$ for RI $> 50\%$, $\pm 25\%$ for RI $> 20\text{--}50\%$, $\pm 30\%$ for RI $> 10\text{--}20\%$, and $\pm 50\%$ for RI
151 $\leq 10\%$ (André et al., 2001). All target ICMs were quantified internally utilizing
152 isotopically labeled surrogate standards. The surrogate standard applied for each analyte
153 is shown in Table 2. At least one lab blank and one lab fortified blank sample utilizing
154 ultrapure water were carried out for every 10 samples. Data acquisition and analysis
155 were conducted with Agilent MassHunter Workstation Software (Ver. B.06.01).
156 For quantification, a calibration curve of at least seven points was constructed over the
157 concentration range of $10\text{--}20000\text{ ng L}^{-1}$ for each ICM with 1000 ng L^{-1} of ILSSs. All
158 target analytes were calibrated internally using linear regression with $1/x$ weighting
159 based on the relative response factors (RRFs) for the analytes and their corresponding
160 isotopically labeled surrogate compound (Table 2). The instrument detection limit (IDL)
161 was determined as the minimum injected mass (ng) that yielded into a signal to noise
162 ratio (S/N) of > 3 . The method detection limit (MDL) was driven by processing seven
163 fortified replicates at concentration 2-5 times the estimated IDL. The MDL was
164 computed as the product of the standard deviation of the measured concentrations and
165 the student's t critical value for the 99% of confidence level with 6 degrees of freedom
166 (for seven replicate determinations the t-value is 3.143) (Kirchmer, 1982).
167 Recovery experiments were carried out utilizing tap water, groundwater and secondary
168 effluent. Five fortified replicate samples were prepared by spiking 100 ng L^{-1} of seven
169 ICMs into each water matrix. The recovery was computed as the difference between the
170 measured concentration in the fortified and unfortified sample divided by the fortified
171 concentration times one hundred in order to express as a percentage.

172

173 **1.5. UV dose determination on collimated beam device**

174

175 A collimated beam UV device (CBD 11-1, ITT Wedeco) equipped with 4 LP-UV Hg
176 lamps (NLR2036, radiation flux of 9 watts) that produces a monochromatic light at a
177 wavelength of 253.7 nm was used for this experiment. The UV irradiance was
178 determined by a calibrated UV detector (SED 240, international light) coupled to a
179 radiometer (IL 1700, International Light). These values were adjusted by correction
180 factors based on Bolton & Linden (2003) on the equation (1):

181

$$182 \quad E' = E_0 \times PF \times RF \times WF \times DF \quad (1)$$

183

184 Where E' is the weighted average UV irradiance (mW cm^{-2}); E_0 is the radiometer
185 measurement at the surface area of the liquid within the Petri dish and at the center of
186 the UV beam collimated device (mW cm^{-2}); PF is the Petri factor (non-uniformity of
187 incident fluence rate across the dish area); RF is the reflection factor (small portion of
188 the beam light which is reflected off the media); WF is the water factor (decrease of the
189 irradiance due to the distance between light source and solution); and DF is the
190 divergence factor (decrease of the UV beam due to the distance between the light source
191 and surface media).

192

$$193 \quad \text{UV dose} = E' \times t \quad (2)$$

194

195 The irradiance value calculated in the water is used as the average fluence rate (mW cm^{-2}).
196 The inverse of this number is the t value, exposure time (s), which was used to obtain
197 the UV dose (mJ cm^{-2}) by multiplying the exposure time by the UV irradiance E' . The
198 LP UV dosage or fluence, used in this study were 0, 100, 200, 400, 600 and 800 mJ cm^{-2} .
199

200 Briefly, 200 mL of the prepared sample (groundwater spiked with ICMs) was
201 transferred to a crystallization petri dish (inner diameter 12.5 cm) and sodium
202 hypochlorite was added. For each sample, 10 mL was taken out to measure the
203 concentration of free chlorine by a Hatch colorimeter immediately before and after UV
204 irradiation. The remaining volume was then aliquoted for the ICMs analysis. This was
205 repeated for the UV/H₂O₂ experiments, where H₂O₂ concentrations were measured
206 using a hydrogen peroxide colorimeter kit I-2016 (CHEMetrics) both before and after
207 UV irradiation. The remaining volume was also aliquoted for ICMs analysis. To ensure
208 that the oxidant reaction time was equal to the UV irradiation exposure time, an excess
209 amount of sodium sulfite was prepared to quench the free chlorine and monochloramine
210 after UV irradiation.

211

212 **3. Results**

213

214 **3.1 Optimization for liquid chromatography conditions**

215

216 To maximize separation efficiently of the seven target ICMs, Agilent Poroshell 120 EC-
217 C8 column (4.6×100 mm, 2.7 μm particle size) was chosen, while water containing
218 0.1% (v/v) formic acid and methanol containing 0.1% (v/v) formic acid were applied as
219 mobile phases. As shown in Fig. 1, under the optimized LC conditions, baseline
220 separation was achieved for the isomers—DTZ and IOT, which were difficult to
221 separate (Ens et al., 2014). Also, the two stereoisomers of IOP were separated.
222 However, since no single standards were available for IOP stereoisomers, the two peaks
223 were combined to quantify the concentration of IOP.

224

225 [Fig. 1]

226

227 3.2. Method linearity and limits of detection

228

229 The DI LC-MS/MS method was validated utilizing drinking water, groundwater and
230 secondary effluent spiked with 200 ngL⁻¹ of target ICM into each water matrix by seven
231 replicates. The recovery for target ICMs was 86 to 100% in drinking water, 85 to 103%
232 in groundwater and 84 to 105% in WWTP effluent. A ten-point calibration curve was
233 prepared in MQ water ranging from 20-20000 ng L⁻¹ in order to test LC-MS/MS
234 response. Calibration curves for target ICMs had good linearity (R²>0.996). As shown
235 in Table 3, IDLs for target ICMs ranged from 0.5-1.5 ng L⁻¹, and MDLs ranged from
236 0.7-21 ng L⁻¹ in ultra pure water. The work of chromatographic separation is shown in
237 Fig 2.

238

239 [Table 3]

240

241 [Fig. 2]

242

243 3.3. Removal of ICM during LPUV/H₂O₂, LPUV/Cl₂ and LPUV/NH₂Cl 244 treatment

245

246 A pseudo-first order kinetics was observed for the degradation of seven ICMs and
247 plotted by linear relations between ln([C]/[C₀]) versus UV dose (mJ cm⁻²) during UV
248 exposure (0, 100, 200, 400, 600 and 800 mJ cm⁻²) with an addition of 0, 3.5 and 7 mg
249 L⁻¹ of hydrogen peroxide and 0, 2.5 and 5 mg L⁻¹ of free chlorine and monochloramine

250 respectively. Since the fluence (mJ cm^{-2}) delivered into the sample is the product of the
 251 exposure time (s) and the fluence rate (mW cm^{-2}) at the same wavelength range, Eq (3)
 252 is equivalent to Eq (4) (Wang et al.,2012). From the slope of each plot, the apparent rate
 253 constant for each condition were determined experimentally

254

$$255 \quad \ln\left(\frac{C}{C_0}\right)_{\text{UV-OXI}} = -K_{\text{UV-OXI}}t = -(K_{\text{UV}} + K_{\text{OXI}})t \quad (3)$$

$$256 \quad \ln\left(\frac{C}{C_0}\right)_{\text{UV-OXI}} = -K_{\text{UV-OXI}}f = -(K_{\text{UV}} + K_{\text{OXI}})f \quad (4)$$

257

258 Where C_0 and C are the concentration of ICMs before and after the treatment, the K_{oxi}
 259 represents different oxidants (i.e. H_2O_2 , Cl_2 , and NH_2Cl) at different concentrations
 260 explained above, and f is the fluence rate. The direct photolysis linear plots of
 261 $\ln[C]/[C_0]$ versus fluence (UV dose) for all ionic and non-ionic ICMs are shown in Fig.
 262 3. Generally, the addition of H_2O_2 and oxidants such as Cl^- and NH_2Cl during UV
 263 treatment can significantly improve the degradation of organic contaminants due to the
 264 contribution of $\bullet\text{OH}$, $\bullet\text{Cl}$ and $\bullet\text{NHCl}$ (Buxton & Ross, 1988; Fang & Shang, 2014;
 265 Patton et al., 2017). However, the addition of each oxidant did not promote an extent in
 266 the attenuation of target ICMs, which indicates UV direct photolysis is the primary
 267 mechanism to attenuate these photolabile organic compounds. Table 3 shows fluence
 268 decay apparent rate constant. Even at UV doses of 100 mJ cm^{-2} without additional of
 269 oxidants, 37% attenuation was observed. Furthermore, the formation of $\bullet\text{OH}$ did not
 270 appreciably promote the attenuation of photo-susceptible ICMs during AOP treatment,
 271 which could be due to rapid degradation attributed from direct photolysis (Kim &
 272 Tanaka, 2009; Pereira & Singer, 2007).

273

274

[Table 4]

275 **[Fig. 3]**

276

277

278 The photo-degradability performance relies mainly on two compound-specific features
279 such as the quantum yield (ϕ) at specific wavelength (λ) and the molar absorption
280 coefficient (ϵ) to which it is exposed (Sanches & Pereira, 2010; Tian et al., 2014). The
281 quantum yield is the ratio between decomposed molecules and the total numbers of
282 photons absorbed by the compound, while the molar absorption coefficient is a
283 measurement of the capacity of a compound to absorb light at a specific wavelength
284 from the UV spectrum. Even the use of low UV doses can promote the degradation of
285 photolabile organic compounds by direct photolysis due to their potential to absorb
286 light. Therefore, the abatement of all ICMs by direct photolysis was mainly associated
287 to the photochemical reaction since more photons are absorbed.

288

289 **[Table 5]**

290

291 Since aqueous hydrogen peroxide, free chlorine, and monochloramine components have
292 different extinction coefficient at 254 nm, when samples are exposed to LPUV, the
293 fraction of UV absorbed by the sample is different in each case. Thus, different pseudo
294 first order decay constant can be obtained. The average removal of ICM under each
295 treatment is presented ahead. As shown in Fig. 3, increasing the UV dose increase the
296 destruction of target ICM. Nevertheless, increasing the oxidants dose (hydrogen
297 peroxide and free chlorine) does not enhance ICM removal. This could be due to their
298 high product of molar absorption coefficient and quantum yield. This yields in the very
299 high photo-degradability compound, neglecting the need of oxidants to the extent the

300 removals (Allard et al., 2016; Yu et al., 2015). Table 5 shows basic properties of ICMs
301 along with molar absorption and quantum yield.

302

303 **4. Conclusion**

304

305 This direct injection method yielded lower method detection limits of 0.7-21 ng L⁻¹ and
306 recoveries above 95% in groundwater, drinking water and secondary effluent.
307 Validation experiments under LPUV illustrated that direct photolysis is the main
308 mechanism to attenuate seven target ICM in groundwater. Oxidants such as hydrogen
309 peroxide, free chlorine and monochloramine did not enhance the removal of ICM. The
310 use of free chlorine and monochloramine as a radical under AOP may have some
311 adverse consequence such as the formation of a variety of iodinated disinfection by
312 products of low-high molecular weight that are still unknown.

313

314 **5. Acknowledgments**

315

316 The authors would like to acknowledge The University of Arizona, Department of
317 Chemical and Environmental engineering for providing the facility for UV experiments.
318 We especially wish to acknowledge Xylem Wedeco for providing collimated beam
319 device low-pressure ultra violet light reactor. We also appreciate Agilent Technologies
320 for their assistance with the acquisition and maintenance of the instrumentation used in
321 this study.

322

323 **6. References:**

324 Allard, S., Criquet, J., Prunier, A., Falantin, C., Le Person, A., Yat-Man Tang, J., Croué,

325 J.P., 2016. Photodecomposition of iodinated contrast media and subsequent
326 formation of toxic iodinated moieties during final disinfection with chlorinated
327 oxidants. *Water Res.* 103, 453–461. <https://doi.org/10.1016/j.watres.2016.07.050>

328 André, F., De Wasch, K.K.G., De Brabander, H.F., Impens, S.R., Stolker, L.A.M., Van
329 Ginkel, L., Stephany, R.W., Schilt, R., Courtheyn, D., Bonnaire, Y., Fürst, P.,
330 Gowik, P., Kennedy, G., Kuhn, T., Moretain, J.P., Sauer, M., 2001. Trends in the
331 identification of organic residues and contaminants: EC regulations under revision.
332 *TrAC - Trends Anal. Chem.* 20, 435–445. [https://doi.org/10.1016/S0165-](https://doi.org/10.1016/S0165-9936(01)00085-1)
333 [9936\(01\)00085-1](https://doi.org/10.1016/S0165-9936(01)00085-1)

334 Bolton, J.R., Linden, K.G., 2003. Standardization of methods for fluence (UV dose)
335 determination in bench-scale UV experiments. *J. Environ. Eng.* 129, 209–215.
336 [https://doi.org/10.1061/\(ASCE\)0733-9372\(2003\)129:3\(209\)](https://doi.org/10.1061/(ASCE)0733-9372(2003)129:3(209))

337 Buseti, F., Linge, K.L., Blythe, J.W., Heitz, A., 2008. Rapid analysis of iodinated X-
338 ray contrast media in secondary and tertiary treated wastewater by direct injection
339 liquid chromatography-tandem mass spectrometry. *J. Chromatogr. A* 1213, 200–
340 208. <https://doi.org/10.1016/j.chroma.2008.10.021>

341 Buxton, G. V., Greenstock, C.L., Helman, W.P., Ross, A.B., 1988. Critical Review of
342 rate constants for reactions of hydrated electrons, hydrogen atoms and hydroxyl
343 radicals ($\cdot\text{OH}/\cdot\text{O}$ —in Aqueous Solution. *J. Phys. Chem. Ref. Data* 17, 513–886.
344 <https://doi.org/10.1063/1.555805>

345 Duirk, S.E., Lindell, C., Cornelison, C.C., Kormos, J., Ternes, T.A., Attene-Ramos, M.,
346 Osiol, J., Wagner, E.D., Plewa, M.J., Richardson, S.D., 2011. Formation of toxic
347 iodinated disinfection by-products from compounds used in medical imaging.
348 *Environ. Sci. Technol.* 45, 6845–6854. <https://doi.org/10.1021/es200983f>

349 Ens, W., Senner, F., Gygax, B., Schlotterbeck, G., 2014. Development, validation, and

350 application of a novel LC-MS/MS trace analysis method for the simultaneous
351 quantification of seven iodinated X-ray contrast media and three artificial
352 sweeteners in surface, ground, and drinking water. *Anal. Bioanal. Chem.* 406,
353 2789–2798. <https://doi.org/10.1007/s00216-014-7712-0>

354 Fang, J., Fu, Y., Shang, C., 2014. The roles of reactive species in micropollutant
355 degradation in the UV/free chlorine system. *Environ. Sci. Technol.* 48, 1859–1868.
356 <https://doi.org/10.1021/es4036094>

357 Kim, I., Yamashita, N., Tanaka, H., 2009. Photodegradation of pharmaceuticals and
358 personal care products during UV and UV/H₂O₂ treatments. *Chemosphere* 77,
359 518–525. <https://doi.org/10.1016/j.chemosphere.2009.07.041>

360 Kirchmer, C.J., 1982. Trace analyses for wastewaters. *Environ. Sci. Technol.* 16, 430A.
361 <https://doi.org/10.1021/es00102a706>

362 Patton, S., Li, W., Couch, K.D., Mezyk, S.P., Ishida, K.P., Liu, H., 2017. Impact of the
363 ultraviolet photolysis of monochloramine on 1,4-dioxane removal: New insights
364 into potable water reuse. *Environ. Sci. Technol. Lett.* 4, 26–30.
365 <https://doi.org/10.1021/acs.estlett.6b00444>

366 Pauwels, B., Verstraete, W., 2006. The treatment of hospital wastewater: An appraisal.
367 *J. Water Health* 4, 405–416. <https://doi.org/10.2166/wh.2006.025>

368 Pereira, V.J., Weinberg, H.S., Linden, K.G., Singer, P.C., 2007. UV degradation
369 kinetics and modeling of pharmaceutical compounds in laboratory grade and
370 surface water via direct and indirect photolysis at 254 nm. *Environ. Sci. Technol.*
371 41, 1682–1688. <https://doi.org/10.1021/es061491b>

372 Pérez, S., Barceló, D., 2007. Fate and occurrence of X-ray contrast media in the
373 environment. *Anal. Bioanal. Chem.* 387, 1235–1246.
374 <https://doi.org/10.1007/s00216-006-0953-9>

375 Richardson, S.D., Fasano, F., Ellington, J.J., Crumley, F.G., Buettner, K.M., Evans, J.J.,
376 Blount, B.C., Silva, L.K., Waite, T.J., Luther, G.W., Mckague, A.B., Miltner, R.J.,
377 Wagner, E.D., Plewa, M.J., 2008. Occurrence and mammalian cell toxicity of
378 iodinated disinfection byproducts in drinking water. *Environ. Sci. Technol.* 42,
379 8330–8338. <https://doi.org/10.1021/es801169k>

380 Sacher, F., Raue, B., Brauch, H.J., 2005. Analysis of iodinated X-ray contrast agents in
381 water samples by ion chromatography and inductively-coupled plasma mass
382 spectrometry. *J. Chromatogr. A* 1085, 117–123.
383 <https://doi.org/10.1016/j.chroma.2005.01.031>

384 Sanches, S., Barreto Crespo, M.T., Pereira, V.J., 2010. Drinking water treatment of
385 priority pesticides using low pressure UV photolysis and advanced oxidation
386 processes. *Water Res.* 44, 1809–1818. <https://doi.org/10.1016/j.watres.2009.12.001>

387 Tarun Anumol, Shimin Wu, S.M. and S.S., 2013. Analysis of Trace Organic
388 Contaminants in Water by Direct Injection Using Agilent 6490 LC / MS / MS with
389 Pos / Neg. Appl. note, *Environ. Agil.* 1–10.

390 Ternes, T.A., Bonerz, M., Herrmann, N., Löffler, D., Keller, E., Lacida, B.B., Alder,
391 A.C., 2005. Determination of pharmaceuticals, iodinated contrast media and musk
392 fragrances in sludge by LC tandem MS and GC/MS. *J. Chromatogr. A* 1067, 213–
393 223. <https://doi.org/10.1016/j.chroma.2004.10.096>

394 Ternes, T.A., Hirsch, R., 2000. Occurrence and behavior of X-ray contrast media in
395 sewage facilities and the aquatic environment. *Environ. Sci. Technol.* 34, 2741–
396 2748. <https://doi.org/10.1021/es991118m>

397 Tian, F.X., Xu, B., Lin, Y.L., Hu, C.Y., Zhang, T.Y., Gao, N.Y., 2014.
398 Photodegradation kinetics of iopamidol by UV irradiation and enhanced formation
399 of iodinated disinfection by-products in sequential oxidation processes. *Water Res.*

400 58, 198–208. <https://doi.org/10.1016/j.watres.2014.03.069>

401 Wang, D., Bolton, J.R., Hofmann, R., 2012. Medium pressure UV combined with
402 chlorine advanced oxidation for trichloroethylene destruction in a model water.
403 Water Res. 46, 4677–4686. <https://doi.org/10.1016/j.watres.2012.06.007>

404 Weissbrodt, D., Kovalova, L., Ort, C., Pazhepurackel, V., Moser, R., Hollender, J.,
405 Siegrist, H., Mcardell, C.S., 2009. Mass flows of x-ray contrast media and
406 cytostatics in hospital wastewater. Environ. Sci. Technol. 43, 4810–4817.
407 <https://doi.org/10.1021/es8036725>

408 Westerhoff, P., Yoon, Y., Snyder, S., Wert, E., 2005. Fate of endocrine-disruptor,
409 pharmaceutical, and personal care product chemicals during simulated drinking
410 water treatment processes. Environ. Sci. Technol. 39, 6649–6663.
411 <https://doi.org/10.1021/es0484799>

412 Yu, H.-W., Anumol, T., Park, M., Pepper, I., Scheideler, J., Snyder, S.A., 2015. On-line
413 sensor monitoring for chemical contaminant attenuation during UV/H₂O₂
414 advanced oxidation process. Water Res. 81, 250–260.
415 <https://doi.org/10.1016/j.watres.2015.05.064>

416

417

A direct injection liquid chromatography tandem mass spectrometry method for
the kinetic study on iodinated contrast media (ICMs) removal in natural water

TABLES

Table 1 Summary of different methods for quantification of ICMs

Compound	Separation & detection	Recovery (%)	Level of detection (ng L ⁻¹)	Reference
IOD, IOP, DTZ, IOT, IOX, IOM	SPE-LC-(+)-ESI-MS-MS	70 % (surface water)	10-30	(Ternes and Hirsch, 2000)
DTZ, ITA, IXA, IOD, IOM, IOP	SPE-LC-(+)-ESI-MS-MS	63-74% (tap water and WWTP effluent)	10-50	(Hirsch et al., 2000)
DTZ, IOP, IOT, IOX	SPE-LC-(+)-ESI-MS-MS	DTZ: 100% OP:100% IOT:55% IOX:90%	50	(Putschew et al., 2001)
DTZ, ITA, IXA, IOD, IOM, IOP, IOX	LC-(+)-ESI-MS-MS	DTZ:97% ITA:98% IXA:98% IOD:109% IOM:96% IOP:98% IOX:99% (surface water and drinking water)	110-210	(Sacher et al., 2001)
IOD, IOM, IOX, DTZ, IOT, IOP, IXA, IDP	LC-(+)-ESI-MS-MS	100-108% 93-102% (MQ water and WWTP effluent)	IOD: 222, IOM: 730, IOX:800, DTZ:830, ITA:970, IOP:200, IXA:110, IDP:110	(Busetti et al., 2008)
IOH, IOM, IOD, IOP, IOX, DTZ	IC-ICP-MS	94-103% 94-109% (Tap water and surface water)	IOH:70, IOM:100, IOD: 120, IOP:130, IOX:110, DTZ:120	(Sacher et al., 2005)
IOH, DTZ, IDP	LC-UV	92-116% (MQ water and tap water)	50,000	(Borowska et al., 2015)
IOD	LC-UV	--	5000	(Tian et al., 2014)

IOD: iopamidol. IOH: iohexol, IOM: iomeprol, IOP: iopromide, IDP: iodipamide, DTZ:

diatrizoate, IOX: ioxitalamic acid, IOT: iothalamic acid, IXA: ioxaglic acid

Table 2 Optimized MRM conditions of target ICM and surrogate standards.

Compound	Abbr.	RT (min)	Surrogate	Prec Ion	Prod Ion	CE (V)	ESI Mode
Assignment							
Iopamidol	IOD	5.64	IOD-d3	777.9	558.7	28	Positive
				777.9	387.0	44	Positive
Ioxitalamic acid	IOX	6.19	IOD-d3	644.8	301.9	48	Positive
				644.8	428.8	28	Positive
Diatrizoic acid	DTZ	7.15	IOH-d5	614.8	233.0	52	Positive
				614.8	361.0	20	Positive
Iothalamic acid	IOT	7.51	IOH-d5	614.8	360.9	28	Positive
				614.8	177.1	56	Positive
Iohexol	IOH	7.58	IOH-d5	821.9	803.8	20	Positive
				821.9	375.0	56	Positive
Iomeprol	IOM	7.73	IOH-d5	777.9	404.9	48	Positive
				777.9	531.8	32	Positive
Iopromide *	IOP	9.77 &	IOH-d5	791.9	572.8	28	Positive
		10.20		791.9	299.8	60	Positive
Surrogate							
Iopamidol-d3	IOD-d3	5.62	–	781.0	562.0	22	Positive
Iohexol-d5	IOH-d5	7.56	–	826.9	810.0	20	Positive

* two isomer peaks

RT: retention time; Prec: Precursor; Prod: product; CE: collision energy

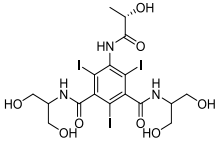
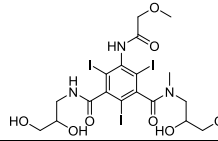
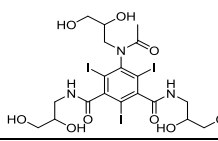
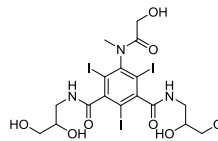
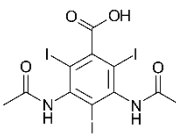
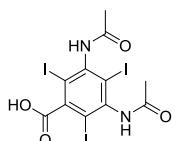
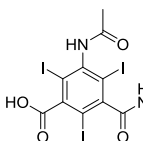
Table 3 Linearity, IDLs, MDLs and recovery for target ICMs

Compound	R ²	IDLs (ng L ⁻¹)	MDLs (ng L ⁻¹)	Recovery (% , n=7)		
				Drinking water	Ground water	WWTP Effluent
IOD	0.9960	0.5	3.1	92±5	97±3	94±4
IOX	0.9996	0.5	6.2	90±6	85±3	84±4
DTZ	0.9988	1.5	15	97±4	99±2	101±2
IOT	0.9997	1.5	21	100±3	103±2	105±3
IOH	0.9987	0.5	5.4	86±4	87±6	85±5
IOM	0.9996	0.5	4.5	92±3	91±4	96±4
IOP	0.9996	0.1	0.7	99±3	100±3	103±4

Table 4 Fluence-based decay apparent rate constant ($10^{-3} \text{ cm}^2 \text{ mJ}^{-1}$) by LPUV treatment along different oxidants at different concentrations

	IOD	IOX	DTZ	IOT	IOH	IOM	IOP
K _{UV}	3.3	3.3	3.5	3.2	3.3	3.1	3.0
K _{UV-H2O2-3.5}	3.7	3.6	3.8	3.4	3.9	3.6	3.6
K _{UV-H2O2-7}	4.0	3.7	3.9	3.6	4.3	4.0	3.9
K _{UV-Cl-2.5}	3.6	3.4	3.8	3.4	3.4	3.1	3.1
K _{UV-Cl-5}	3.6	3.5	3.8	3.4	3.8	3.2	3.3
K _{UV-NH2-2.5}	3.3	3.3	3.5	3.2	3.5	3.1	3.0
K _{UV-NH2-5}	3.4	3.4	3.5	3.3	3.5	3.1	3.2

Table 5 Basic properties of target ICMs with molar absorptivity and quantum yield at 254 nm

Name	Molecular Weight and Formula	Structure	Water Solubility (g/L) ^a	Log Kow ^b	Molar absorption ^c ϵ_{254}	Quantum yield ^d Φ_{254}
lopamidol (IOD)	777.09 $C_{17}H_{22}I_3N_3O_8$		134	-1.38	22	3.4
lopromide (IOP)	791.12 $C_{18}H_{24}I_3N_3O_8$		287	-2.49	22.1	3.9
lohexol (IOH)	821.14 $C_{19}H_{26}I_3N_3O_9$		1000	-2.81	27.7	4.1
lomeprol (IOM)	777.09 $C_{17}H_{22}I_3N_3O_8$		427	-1.35	20	N.A.
Diatrizoic acid (DTZ)	613.92 $C_{11}H_8I_3N_2O_4$		1000	1.37	15.9	7.1
lothalamic acid (IOT)	613.92 $C_{11}H_9I_3N_2O_4$		1000	1.47	19.1	3.8
loxitalami c acid (IOX)	643.94 $C_{12}H_{11}I_3N_2O_5$		1000	0.50	N.A.	N.A.

^a from ACD/Labs 6.0; ^b from KowWIN v1.68; ^c (10^3) ($M^{-1} cm^{-1}$); ^d (10^{-2}) (mol Einstein⁻¹)

N.A.= Not available

FIGURES

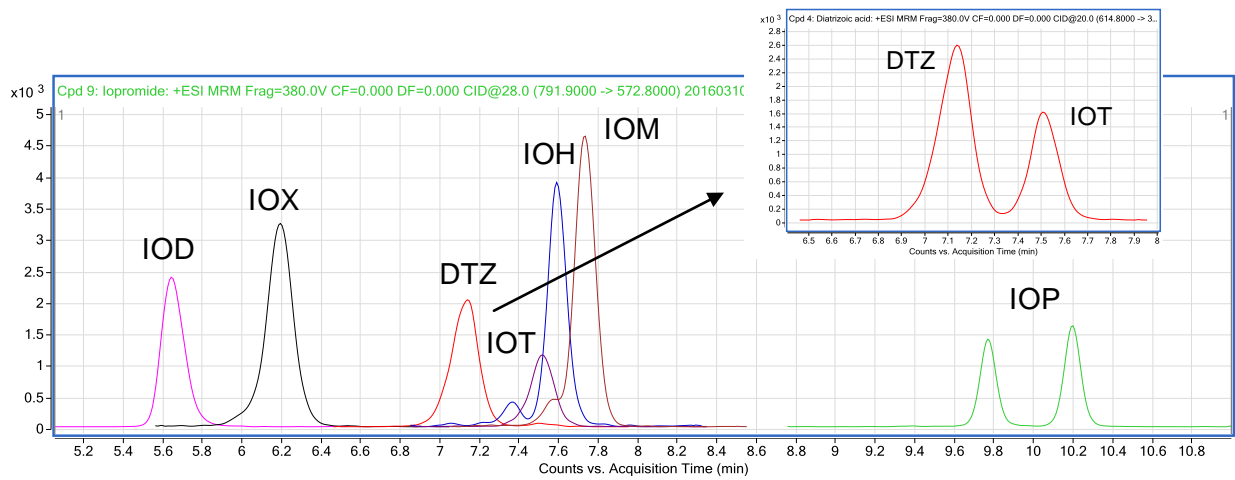


Fig. 1 LC-MS/MS Chromatogram of seven target ICM at 500 ng L⁻¹.

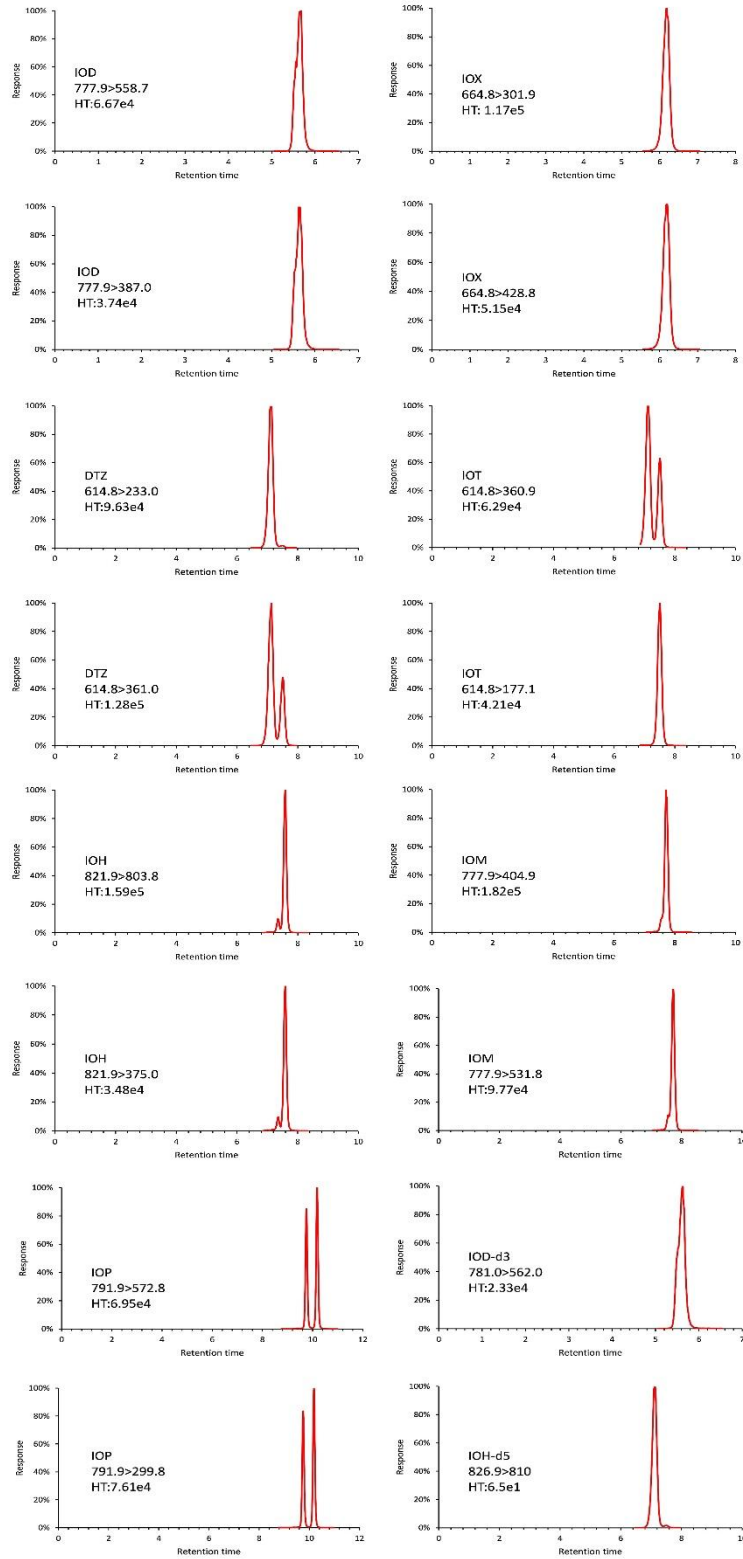


Fig 2 LC-MS/MS chromatogram of all analytes at $20\mu\text{g L}^{-1}$ and surrogate standards at $10\mu\text{g L}^{-1}$ (HT is the counts of height peak).

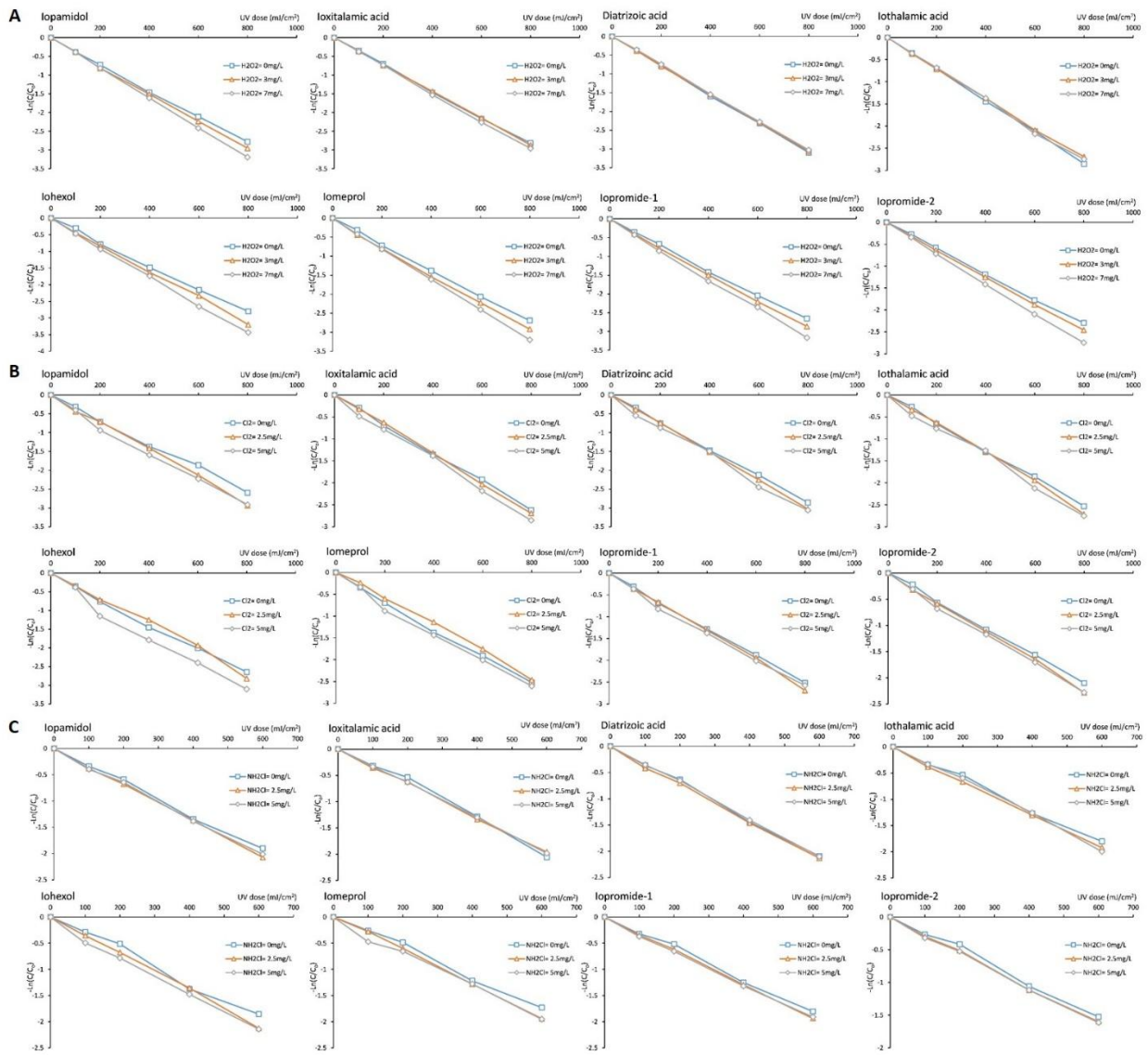


Fig. 3 ICMs attenuation through LPUV A) H₂O₂ B) Cl₂ and C) NH₂Cl